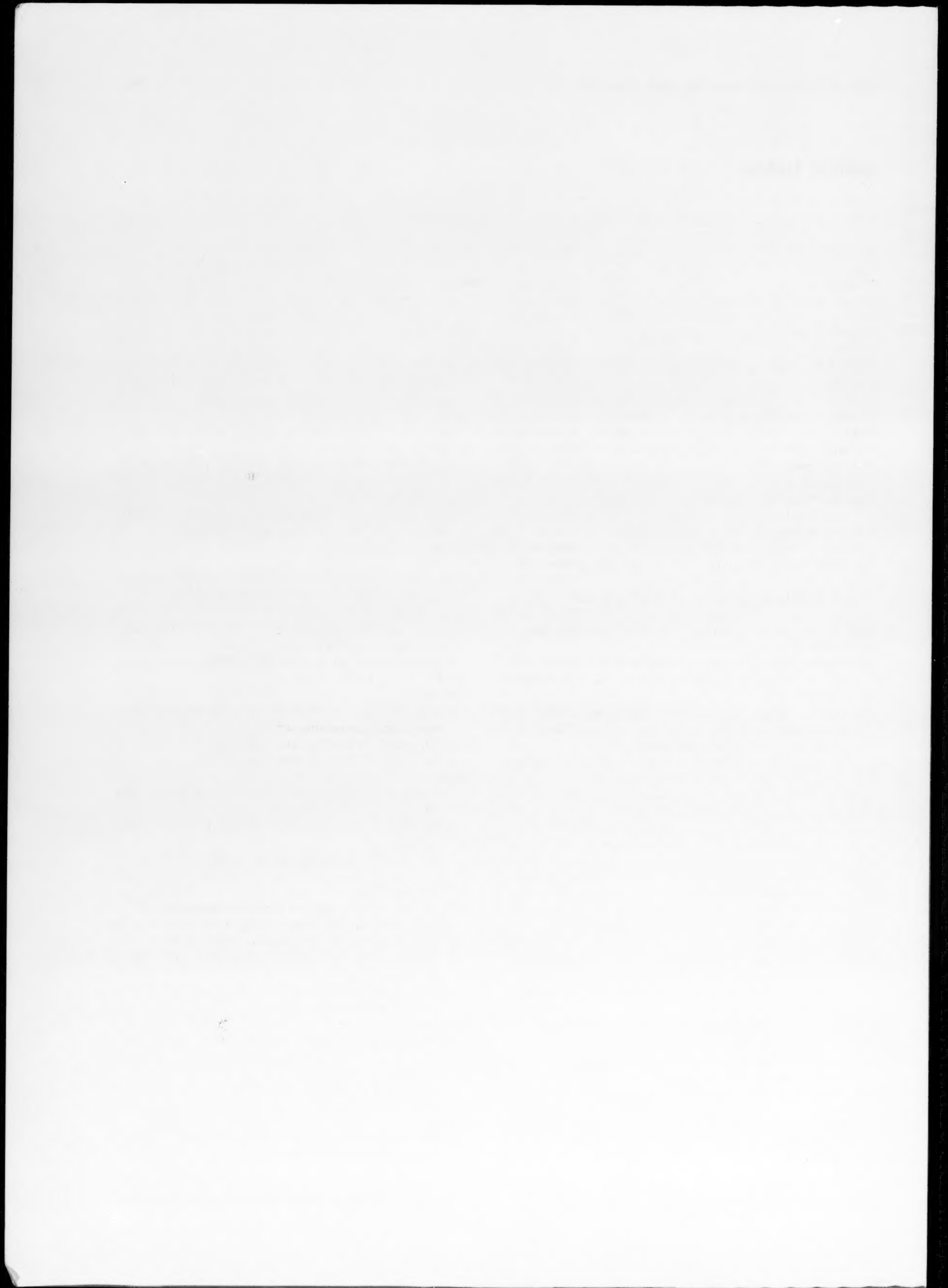


## Author Index

---

- Aballe, M., 231  
Adeva, P., 231  
Arone, R., 15  
Asthana, R., 253
- Bangert, U., 39  
Baudalet, B., 33  
Bieler, T. R., 171  
Botstein, O., 15
- Caceres, C. H., 147  
Calka, A., 107  
Cantor, B., 209  
Charsley, P., 39  
Chen, G., 33  
Conrad, J. R., 259
- Dodd, R. A., 259
- Engelman, H., 107
- Francis, R., 271
- Gan, D., L1  
González-Carrasco, J. L., 231  
Grujicic, M., 201
- Hong, S. I., 55, 155  
Hu, S., 33  
Huang, Z. H., L13
- Jain, M., 183
- Kattamis, T. Z., 241  
Kim, S. J., 217  
Kumosa, M., 45
- Laird, C., 55, 155, L9  
Langdon, T. G., 1  
Lee, Y. T., 77  
Lees, D. G., 271  
Lerf, R., 119  
Lescano, D. E., 147  
Lin, C. L., L1  
Lin, T. L., 23  
Llanes, L., L9
- Maehara, Y., 1  
Magnin, T., 99  
Martin, J. W., 113, 141  
Morris, D. G., 119  
Mukherjee, A. K., 171
- Nagai, H., 195  
Nicholls, D. J., 141
- Oikawa, H., 195  
Ovid'ko, I. A., L5
- Pabi, S. K., 253  
Pak, H. R., 129
- Pak, J. S. L., 129  
Pieraggi, B., 269  
Pogany, A. P., 107
- Rapp, R. A., 269  
Rebiere, M., 99  
Rigsbee, J. M., 129  
Rozenak, P., 91
- Shanks, R. A., 107  
Shen, H., 33  
Shen, P., L1  
Shpigler, B., 15  
Sridharan, K., 259  
Suganuma, T., 241
- Takahashi, T., 195  
Tian, J. F., L13
- Wang, Z. G., L13  
Wayman, C. M., 129, 217  
Welsch, G., 77  
Wen, M., 23  
Wojnar, L., 45  
Worzala, F. J., 259
- Xia, X., 113
- Zhang, D. L., 209



## Subject Index

- Alloying**  
 high strain superplastic deformation mechanisms of mechanically alloyed aluminum IN9021 1, 171  
 mechanical alloying of Al-Ti alloys, 119
- Alloys**  
 corrosion fatigue mechanisms of an 8090 Al-Li-Cu alloy, 99  
 effect of refractory elements on the evolution of the NiAl intermetallic phase in Ni-Cr-Al alloys, 231  
 elevated temperature nitrogen ion implantation of Incoloy alloys 908 and 909 using the plasma source ion implantation process, 259  
 mechanical alloying of Al-Ti alloys, 119  
 precipitation behavior and microstructural changes in maraging Fe-Ni-Mn-Ti alloys, 217  
 superplasticity of steels and ferrous alloys, 1  
 Young's modulus and damping of Ti-6Al-4V alloy as a function of heat treatment and oxygen concentration, 77
- Aluminium**  
 corrosion fatigue mechanisms of an 8090 Al-Li-Cu alloy, 99  
 cyclic deformation behavior of Cu-16at.%Al single crystals  
 Part II: cyclic hardening and slip band behavior, 55  
 cyclic deformation behavior of Cu-16at.%Al single crystals  
 Part III: friction stress and back stress behavior, 155  
 effect of magnesium on the heterogeneous nucleation of cadmium solidification by aluminium, 209  
 effect of refractory elements on the evolution of the NiAl intermetallic phase in Ni-Cr-Al alloys, 231  
 effects of grain size on creep behavior of Ti-50mol.%Al intermetallic compound at 1100 K, 195  
 effects of stretch and heat treatment on microstructure and mechanical properties of an Al-Li-Cu-Mg-Zr alloy, 113  
 examination of the reasons for the discrepancy between long and small fatigue cracks in Al-Li alloys, 141  
 fabrication of the D0<sub>22</sub>-type intermetallic compound Al<sub>3</sub>Ta via powder metallurgy processes and its characterization, 129  
 fatigue crack growth mechanisms in Al-SiC particulate metal matrix composites, 15  
 growth of artificial voids during superplastic deformation of a Zn-Al-Cu alloy, 147  
 high strain superplastic deformation mechanisms of mechanically alloyed aluminium IN9021, 171  
 mechanical alloying of Al-Ti alloys, 119  
 Young's modulus and damping of Ti-6Al-4V alloy as a function of heat treatment and oxygen concentration, 77
- Austenite**  
 design of precipitated austenite for dispersed-phase transformation toughening in high strength Co-Ni steels, 201
- Boron**  
 re-amorphization of crystallized metallic glass Co<sub>70.3</sub>-Fe<sub>4.7</sub>Si<sub>15</sub>B<sub>10</sub> ribbons, 107
- Cadmium**  
 effect of magnesium on the heterogeneous nucleation of cadmium solidification by aluminium, 209
- Carbon**  
 fatigue crack growth mechanisms in Al-SiC particulate metal matrix composites, 15  
 solidification processing and tribological behavior of particulate TiC-ferrous matrix composites, 241
- Characterization**  
 fabrication of the D0<sub>22</sub>-type intermetallic compound Al<sub>3</sub>Ta via powder metallurgy processes and its characterization, 129
- Chromium**  
 effect of refractory elements on the evolution of the NiAl intermetallic phase in Ni-Cr-Al alloys, 231
- Cobalt**  
 design of precipitated austenite for dispersed-phase transformation toughening in high strength Co-Ni steels, 201  
 re-amorphization of crystallized metallic glass Co<sub>70.3</sub>-Fe<sub>4.7</sub>Si<sub>15</sub>B<sub>10</sub> ribbons, 107
- Composites**  
 fatigue crack growth mechanisms in Al-SiC particulate metal matrix composites, 15  
 solidification processing and tribological behavior of particulate TiC-ferrous matrix composites, 241
- Copper**  
 corrosion fatigue mechanisms of an 8090 Al-Li-Cu alloy, 99  
 cyclic deformation behavior of Cu-16at.%Al single crystals  
 Part II: cyclic hardening and slip band behavior, 55  
 cyclic deformation behavior of Cu-16at.%Al single crystals  
 Part III: friction stress and back stress behavior, 155  
 effect of grain size and ramp loading on the low amplitude cyclic stress-strain curve of polycrystalline copper, L9  
 evolution of internal stress variables during cyclic deformation of copper, 183  
 growth of artificial voids during superplastic deformation of a Zn-Al-Cu alloy, 147
- Corrosion**  
 corrosion fatigue mechanisms of an 8090 Al-Li-Cu alloy, 99
- Crack growth**  
 fatigue crack growth mechanisms in Al-SiC particulate metal matrix composites, 15
- Cracks**  
 an examination of the reasons for the discrepancy between long and small fatigue cracks in Al-Li alloys, 141

**Creep**

effects of grain size on creep behavior of Ti-50mol.%Al intermetallic compound at 1100 K, 195

**Damping**

Young's modulus and damping of Ti-6Al-4V alloy as a function of heat treatment and oxygen concentration, 77

**Deformation**

cyclic deformation behavior of Cu-16at.%Al single crystals

Part II: cyclic hardening and slip band behavior, 55

cyclic deformation behavior of Cu-16at.%Al single crystals

Part III: friction stress and back stress behavior, 155

deformation mechanism of a  $\gamma'$  precipitation-hardened nickel-base superalloy, 23

evolution of internal stress variables during cyclic deformation of copper, 183

excited state of solids under shock-wave deformation, L5

growth of artificial voids during superplastic deformation of a Zn-Al-Cu alloy, 147

high strain superplastic deformation mechanisms of mechanically alloyed aluminum IN90211, 171

**Diffusion**

approximate solution for the finite-extent moving-boundary diffusion-controlled dissolution of spheres, 253

**Dislocations**

electron microscope studies of localized changes in dislocation configurations during fatigue, 39

**Dispersion**

design of precipitated austenite for dispersed-phase transformation toughening in high strength Co-Ni steels, 201

**Dissolution**

approximate solution for the finite-extent moving-boundary diffusion-controlled dissolution of spheres, 253

**Electron microscopy**

electron microscope studies of localized changes in dislocation configurations during fatigue, 39

high voltage electron microscopy studies of grain boundary effects on hydrogen embrittlement of stainless steel, 91

**Excited states**

excited state of solids under shock-wave deformation, L5

**Fabrication**

fabrication of the D0<sub>22</sub>-type intermetallic compound Al<sub>3</sub>Ta via powder metallurgy processes and its characterization, 129

**Fatigue**

corrosion fatigue mechanisms of an 8090 Al-Li-Cu alloy, 99

electron microscope studies of localized changes in dislocation configurations during fatigue, 39

examination of the reasons for the discrepancy between long and small fatigue cracks in Al-Li alloys, 141

fatigue crack growth mechanisms in Al-SiC particulate metal matrix composites, 15

**Fractal equations**

comments on some of the fractal equations, 513

**Fracture**

advanced quantitative analysis of fracture surfaces, 45

**Friction**

cyclic deformation behavior of Cu-16at.%Al single crystals

Part III: friction stress and back stress behavior, 155

**Grain boundaries**

high voltage electron microscopy studies of grain boundary effects on hydrogen embrittlement of stainless steel, 91

**Grain size**

effect of grain size and ramp loading on the low amplitude cyclic stress-strain curve of polycrystalline copper, L9

effects of grain size on creep behavior of Ti-50mol.%Al intermetallic compound at 1100 K, 195

**Hardening**

cyclic deformation behavior of Cu-16at.%Al single crystals

Part III: cyclic hardening and slip band behavior, 55

deformation mechanism of a  $\gamma$  precipitation-hardened nickel-base superalloy, 23

**Heat treatment**

effects of stretch and heat treatment on microstructure and mechanical properties of an Al-Li-Cu-Mg-Zr alloy, 113

**Hydrogen**

high voltage electron microscopy studies of grain boundary effects on hydrogen embrittlement of stainless steel, 91

**Hydrogen embrittlement**

high voltage electron microscopy studies of grain boundary effects on hydrogen embrittlement of stainless steel, 91

**Intermetallics**

effect of refractory elements on the evolution of the NiAl intermetallic phase in Ni-Cr-Al alloys, 231

effects of grain size on creep behavior of Ti-50mol.%Al intermetallic compound at 1100 K, 195

fabrication of the D0<sub>22</sub>-type intermetallic compound Al<sub>3</sub>Ta via powder metallurgy processes and its characterization, 129

**Ion implantation**

elevated temperature nitrogen ion implantation of Incoloy alloys 908 and 909 using the plasma source ion implantation process, 259

**Iron**

precipitation behavior and microstructural changes in maraging Fe-Ni-Mn-Ti alloys, 217

re-amorphization of crystallized metallic glass Co<sub>70.3</sub>-Fe<sub>4.7</sub>Si<sub>15</sub>B<sub>10</sub> ribbons, 107

solidification processing and tribological behavior of particulate TiC-ferrous matrix composites, 241

**Lithium**

corrosion fatigue mechanisms of an 8090 Al-Li-Cu alloy, 99

effects of stretch and heat treatment on microstructure and mechanical properties of an Al-Li-Cu-Mg-Zr alloy, 113

examination of the reasons for the discrepancy between long and small fatigue cracks in Al-Li alloys, 141

- Magnesium**  
 effect of magnesium on the heterogeneous nucleation of cadmium solidification by aluminium, 209  
 effects of stretch and heat treatment on microstructure and mechanical properties of an Al-Li-Cu-Mg-Zr alloy, 113
- Manganese**  
 precipitation behavior and microstructural changes in maraging Fe-Ni-Mn-Ti alloys, 217
- Martensite**  
 reverse martensitic transformation in yttria-partially stabilized zirconia with  $\text{TiO}_2$  addition, L1
- Martensitic transformation**  
 reverse martensitic transformation in yttria-partially stabilized zirconia with  $\text{TiO}_2$  addition, L1
- Metallic glasses**  
 re-amorphization of crystallized metallic glass  $\text{Co}_{70.3}\text{Fe}_{4.7}\text{Si}_{15}\text{B}_{10}$  ribbons, 107
- Metals**  
 comments on vacancy annihilation in the growth of scales on metals, 269  
 response to "Comments on vacancy annihilation in the growth of scales on metals", 271
- Microstructure**  
 effects of stretch and heat treatment on microstructure and mechanical properties of an Al-Li-Cu-Mg-Zr alloy, 113  
 precipitation behavior and microstructural changes in maraging Fe-Ni-Mn-Ti alloys, 217
- Moving boundaries**  
 approximate solution for the finite-extent moving-boundary diffusion-controlled dissolution of spheres, 253
- Nickel**  
 deformation mechanism of a  $\gamma'$  precipitation-hardened nickel-base superalloy, 23  
 effect of refractory elements on the evolution of the NiAl intermetallic phase in Ni-Cr-Al alloys, 231  
 precipitation behavior and microstructural changes in maraging Fe-Ni-Mn-Ti alloys, 217  
 transformation toughening in high strength Co-Ni steels, 201
- Nitrogen**  
 elevated temperature nitrogen ion implantation of Incoloy alloys 908 and 909 using the plasma source ion implantation process, 259
- Oxygen**  
 reverse martensitic transformation in yttria-partially stabilized zirconia with  $\text{TiO}_2$  addition, L1
- Phase evolution**  
 effect of refractory elements on the evolution of the NiAl intermetallic phase in Ni-Cr-Al alloys, 231
- Phase transformation**  
 design of precipitated austenite for dispersed-phase transformation toughening in high strength Co-Ni steels, 201
- Plasticity**  
 growth of artificial voids during superplastic deformation of a Zn-Al-Cu alloy, 147
- high strain superplastic deformation mechanisms of mechanically alloyed aluminum IN90211, 171
- Powder metallurgy**  
 fabrication of the  $\text{D0}_{22}$ -type intermetallic compound  $\text{Al}_3\text{Ta}$  via powder metallurgy processes and its characterization, 129
- Precipitation**  
 deformation mechanism of a  $\gamma'$  precipitation-hardened nickel-base superalloy, 23  
 design of precipitated austenite for dispersed-phase transformation toughening in high strength Co-Ni steels, 201  
 precipitation behavior and microstructural changes in maraging Fe-Ni-Mn-Ti alloys, 217
- Ramp loading**  
 effect of grain size and ramp loading on the low amplitude cyclic stress-strain curve of polycrystalline copper, L9
- Re-amorphization**  
 re-amorphization of crystallized metallic glass  $\text{Co}_{70.3}\text{Fe}_{4.7}\text{Si}_{15}\text{B}_{10}$  ribbons, 107
- Refractory elements**  
 effects of refractory elements on the evolution of the NiAl intermetallic phase in Ni-Cr-Al alloys, 231
- Roughening**  
 roughening of the free surfaces of metallic sheets during stretch forming, 33
- Scales**  
 comments on vacancy annihilation in the growth of scales on metals, 269  
 response to "Comments on vacancy annihilation in the growth of scales on metals", 271
- Silicon**  
 fatigue crack growth mechanisms in Al-SiC particulate metal matrix composites, 15  
 re-amorphization of crystallized metallic glass  $\text{Co}_{70.3}\text{Fe}_{4.7}\text{Si}_{15}\text{B}_{10}$  ribbons, 107
- Single crystals**  
 cyclic deformation behavior of Cu-16at.%Al single crystals  
 Part II: cyclic hardening and slip band behavior, 55  
 cyclic deformation behavior of Cu-16at.%Al single crystals  
 Part III: friction stress and back stress behavior, 155
- Slip bands**  
 cyclic deformation behavior of Cu-16at.%Al single crystals  
 Part II: cyclic hardening and slip band behavior, 55
- Solidification**  
 effect of magnesium on the heterogeneous nucleation of cadmium solidification by aluminium, 209  
 solidification processing and tribological behavior of particulate TiC-ferrous matrix composites, 241
- Steels**  
 high voltage electron microscopy studies of grain boundary effects on hydrogen embrittlement of stainless steel, 91  
 superplasticity of steels and ferrous alloys, 1  
 transformation toughening in high strength Co-Ni steels, 201
- Strain**  
 effect of grain size and ramp loading on the low amplitude cyclic stress-strain curve of polycrystalline copper, L9

- high strain superplastic deformation mechanisms of mechanically alloyed aluminum IN90211, 171
- Stress**
- cyclic deformation behavior of Cu-16at.%Al single crystals
    - Part III: friction stress and back stress behavior, 155
  - effect of grain size and ramp loading on the low amplitude cyclic stress-strain curve of polycrystalline copper, L9
  - evolution of internal stress variables during cyclic deformation of copper, 183
- Stretch**
- effects of stretch and heat treatment on microstructure and mechanical properties of an Al-Li-Cu-Mg-Zr alloy, 113
  - roughening of the free surfaces of metallic sheets during stretch forming, 33
- Stretch forming**
- roughening of the free surfaces of metallic sheets during stretch forming, 33
- Superalloys**
- the deformation mechanism of a  $\gamma'$  precipitation-hardened nickel-base superalloy, 23
- Superplasticity**
- superplasticity of steels and ferrous alloys, 1
- Tantalum**
- fabrication of the D0<sub>2</sub>-type intermetallic compound Al<sub>3</sub>Ta via powder metallurgy processes and its characterization, 129
- Titanium**
- effects of grain size on creep behavior of Ti-50mol.%Al intermetallic compound at 1100 K, 195
  - mechanical alloying of Al-Ti alloys, 119
  - precipitation behavior and microstructural changes in maraging Fe-Ni-Mn-Ti alloys, 217
  - reverse martensitic transformation in yttria-partially stabilized zirconia with TiO<sub>2</sub> addition, L1
- solidification processing and tribological behavior of particulate TiC-ferrous matrix composites, 241
- Young's modulus and damping of Ti-6Al-4V alloy as a function of heat treatment and oxygen concentration, 77
- Toughening**
- design of precipitated austenite for dispersed-phase transformation toughening in high strength Co-Ni steels, 201
- Tribology**
- solidification processing and tribological behavior of particulate TiC-ferrous matrix composites, 241
- Vacancy annihilation**
- comments on vacancy annihilation in the growth of scales on metals, 269
  - response to "Comments on vacancy annihilation in the growth of scales on metals", 271
- Vanadium**
- Young's modulus and damping of Ti-6Al-4V alloy as a function of heat treatment and oxygen concentration, 77
- Voids**
- growth of artificial voids during superplastic deformation of a Zn-Al-Cu alloy, 147
- Young's modulus**
- Young's modulus and damping of Ti-6Al-4V alloy as a function of heat treatment and oxygen concentration, 77
- Yttrium**
- reverse martensitic transformation in yttria-partially stabilized zirconia with TiO<sub>2</sub> addition, L1
- Zinc**
- growth of artificial voids during superplastic deformation of a Zn-Al-Cu alloy, 147
- Zirconium**
- reverse martensitic transformation in yttria-partially stabilized zirconia with TiO<sub>2</sub> addition, L1

